

TESLA COLLABORATION

Beam Position Monitors for the TESLA Accelerator Complex

C. Magne, M. Wendt*

CEA Saclay, *DESY



December 2000, TESLA 2000-41

Beam Position Monitors for the TESLA Accelerator Complex

C. Magne
CEA, Saclay, France

M. Wendt
DESY, Hamburg, Germany

December, 2000

Abstract

An overview on beam position monitoring at the TESLA linear collider is given. Basic principles and technology details of BPM pickup's and their read-out electronics are discussed. Experience with different types of BPM systems, made at the TESLA Test Facility Linac, at HERA, and at other accelerators, are considered and lead to the proposed BPM solutions.

1 Introduction

The 500 GeV center-of-mass TESLA e^+/e^- linear collider [1], currently under investigation at DESY, requires *beam position monitors* (BPM) not only in the two 10 km long superconducting main linacs, but in all accelerator subsystems, e.g. injector complex, transport-lines, damping rings, beam delivery system, etc. Also for the integrated X-ray SASE *free electron LASER* (FEL) facility precision BPM's are needed to align the electron beam on the magnetic axes of the undulators.

beam energy	=	2×250 GeV
TESLA rep. rate f_{rep}	=	5 Hz
TESLA macro pulse length t_{pulse}	=	950 μ s
# of bunches per pulse n_b	=	2820 (HEP ^a), 9900 (FEL ^b)
bunch spacing Δt_b	=	337 ns (HEP), 93 ns (FEL)
N_e per bunch	=	2×10^{10} (HEP), 6×10^{10} (FEL)
bunch length σ_z	=	300 μ m (HEP), 25...50 μ m (FEL)

^ahigh-energy physics operation

^bfree-electron laser operation

Table 1: TESLA beam parameters.

Most requirements for the TESLA beam position monitors are deduced from the beam parameters listed in Table 1. In order to realize a true single-bunch beam position measurement the integration (measurement) time of each BPM system (pickup and read-out electronics) has to be < 337 ns. The BPM's in the sections of the FEL undulator have to response within 93 ns. As all 2820 (HEP), 9900 (FEL) bunches are stacked in the 17 km long damping rings, their distance here is much closer. Fortunately a single-bunch capability is not required for the BPM's of the damping rings.

Particular during machine comissioning, lower bunch charges and different macro pulse fill patterns have to be considered. The dynamic range of the BPM read-out electronics has to handle those beam intensity variations.

An overview of the basic BPM installations is shown in Table 2. All vacuum chambers have a circular cross-section, only the dog-bone style arcs of the damping rings will have a beam pipe with elliptic cross-section. Because of the negligible synchrotron light – except along the arcs and

accelerator	# of BPM's	beam pipe radius	required resolution	type of pickup
main linac	2×368	39 mm	$10 \mu\text{m}$	cavity BPM
BDS	2×102	8.5 mm	$1 \mu\text{m}$	stripline
damping ring	2×824	25...50 mm ^a	$1 \mu\text{m}$ ^b	button
FEL-undulators	297	5 mm	$1 \mu\text{m}$	stripline

^aparts of the vacuum system of the damping rings have elliptic cross-section

^bin average mode over many turns

Table 2: BPM installations at TESLA.

at the wiggler of the damping rings – the pickup electrodes can be arranged symmetrically in the horizontal and vertical plane.

The required BPM resolution has to meet the needs of the *beam based alignment* (BBA) procedures to guarantee the beam quality. This leads to a resolution of $\approx 10 \mu\text{m}$ in the superconducting main linacs – assuming an averaging over a “few” bunches (integration time $< 10 \mu\text{s}$) or even a single-bunch position measurement (response time $< 337 \text{ ns}$). For the beam delivery system (BDS) and for the FEL-undulator stripline pickup based BPM's are proposed, which should give a $1 \mu\text{m}$ single-bunch resolution. They will be located inside the quadrupoles to improve the alignment accuracy. Also the damping ring BPM's have to accomplish a resolution of $1 \mu\text{m}$, but here it may be achieved in an average mode over many turns.

BPM's with moderate resolution ($50 \mu\text{m}$) – not listed in Table 2 – are needed for the injector complex and along the transport lines. They will be equipped with button type pickup stations.

All BPM's presented so far will be used for *beam orbit* diagnostics, those in the BDS also for a slow orbit feedback. A few more, very specialized BPM's are required for the *fast luminosity feedback system* in the interaction region (IR) of the BDS.

2 The Basics of Beam Position Monitoring

Each beam position monitor (Figure 1) basically consists out of the pickup station for the signal detection and a set of read-out electronics (often 2 channels for horizontal and vertical plane) for signal processing and *normalization*.

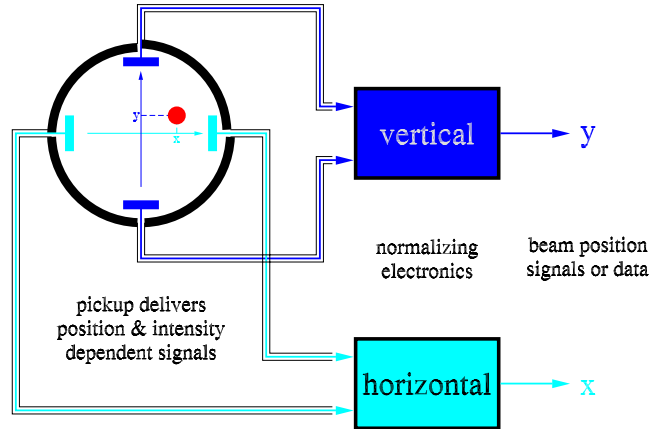


Figure 1: BPM principle.

A single electrode of a BPM pickup delivers a signal voltage

$$V_{\text{elec}}(\omega, x, y) = s(x, y) Z(\omega) I_{\text{beam}}(\omega) \quad (1)$$

which is proportional to the beam intensity $I_{\text{beam}}(\omega)$ (e.g. bunch charge) and to the beam-to-electrode distance (x, y) (e.g. transverse beam displacement), covered by a sensitivity function $s(x, y)$. Because of the quite short $- < 1$ mm long $-$ bunches in TESLA the frequency spectra of $I_{\text{beam}}(\omega)$ is of no concern; for all BPM designs the TESLA bunches are taken as dirac impulse excitation signals. The transfer impedance $Z(\omega)$ depends on the pickup geometry and is given for a centered beam ($x = y = 0$). It fixes (roughly) the frequency range of the following signal processing system.

Two categories of *BPM pickup's* are foreseen for TESLA:

Resonant An off-center beam excites dipol mode resonances in a cavity or waveguide style pickup. This type of BPM offers the steepest slope of $s(x, y)$ and has therefore a high resolution potential. Because of the resonant characteristic of $Z(\omega)$ (high Q value) the single bunch capability cannot be realized without “modifications”, e.g. the damping of the resonances has to be increased, such that the bunch excited oscillations are completely decayed within the bunch-to-bunch spacing (337 ns). This lowering of the Q value may lead to some reduction of the high initial sensitivity.

Broadband Stripline, as well as button pickup's don't resonate and have only little influence on the EM-field of the beam. Therefore the sensitivity $s(x, y)$ of these pickup's can be approximated with the wall current model of the unperturbed beam pipe. Because of the broadband characteristic of $Z(\omega)$, the output signals are pulses with a very short decay time, such that the single bunch capability is not a problem of principle.

The *BPM read-out electronics* extracts the beam position (displacement) information from the analogue signals of the pickup electrodes. In order to simplify the normalization procedure and to reduce the nonlinearities of $s(x, y)$ two symmetrically arranged electrode are sensed in each plane (see Figure 1). The read-out electronics *normalizes* the electrode signals and therefore performs a beam intensity independent beam position measurement. This beam position is usually delivered in a digital format for the horizontal (x) and the vertical (y) plane.

3 BPM Pickup Stations

3.1 Cavity Monitors

The conditions in the two main linacs with their superconducting RF acceleration structures differ quite much from those in all the other subaccelerators of TESLA. Cryogenic temperatures (2 K), *class 10* cleanroom conditions and a large beam pipe aperture require a specialized beam position pickup. Resonant cavity or waveguide structures consist of simple machineable parts and have the highest resolution potential when used for beam position monitoring.

Two types of cavity monitors for beam position measurements have been tested in detail at the TESLA Test Facility (TTF) linac:

3.1.1 Cylindrical RF Cavity BPM

An off-center beam passing a cylindrical RF cavity (sometimes called *pillbox* cavity) excites resonant modes from which the first dipol mode (TM_{110}) is used for beam position monitoring (Figure 2). A pin-antenna, mounted at the location of maximum electric field ($r_{E_{max}} = 0.481 r$), couples out a voltage signal:

$$V_{110}^{out}(\delta x) = V_{110}^{in}(\delta x) \frac{\beta}{1 + \beta} \sqrt{\frac{R_{load}}{Q_L}} = V_{110}^{in}(\delta x) \left(\frac{R}{Q}\right)_{110}^{-\frac{1}{2}} \sqrt{\frac{R_{load}}{Q_L}} \left(1 - \frac{Q_L}{Q_0}\right) \quad (2)$$

in a $R_{load} = 50 \Omega$ system. Here Q_0 and Q_L denote the unloaded and loaded Q-factor of the cavity with the radius r and length l . In the TESLA main linacs particles are relativistic, $\beta = 1$. The

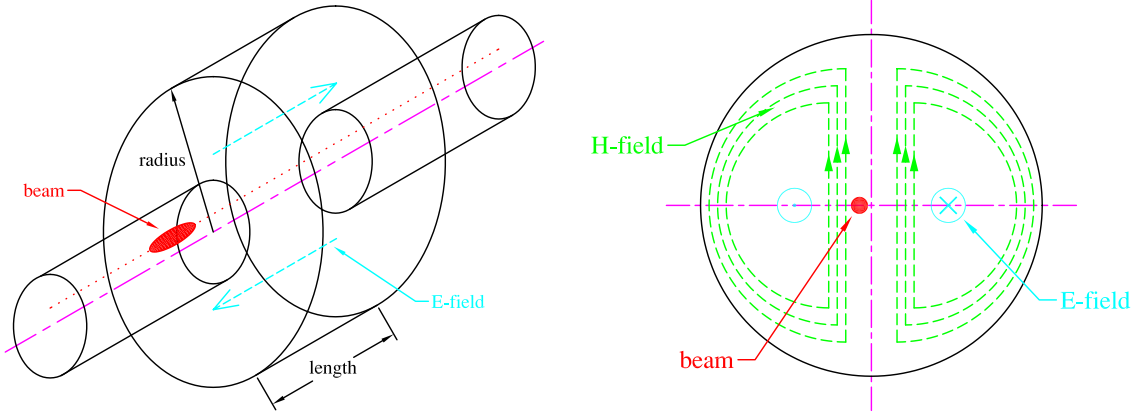


Figure 2: Beam-excited TM_{110} in a cylindrical cavity BPM...
...and the corresponding fields of horizontal polarisation.

R/Q of the TM_{110} -mode is:

$$\left(\frac{R}{Q}\right)_{110} = \frac{2 Z_0 l (J_1^{max})^2 T_{tr}^2}{\pi r J_0^2(a_{11}) a_{11}} \approx 130.73 \frac{l}{r} T_{tr}^2 \quad (3)$$

where a_{11} is the first root of J_1 , $J_1^{max} \approx 0.582$ its maximum and the transit-time factor T_{tr} is given by:

$$T_{tr} = \frac{\sin\left(\frac{\pi l}{\lambda_{mn0}}\right)}{\left(\frac{\pi l}{\lambda_{mn0}}\right)} \quad (4)$$

The induced signal $V_{110}^{in}(\delta x)$ in eq.(2) of a charge q at δx , $\phi = 90^\circ$ computes to:

$$V_{110}^{in}(\delta x) = \frac{2 k_{110} q}{J_1^{max}} J_1\left(\frac{a_{11} \delta x}{r}\right) \quad (5)$$

with $k_{110} = (\omega/2) (R/Q)_{110}$. More theoretical aspects are found in [2]. For the cavity BPM's tested at the TTF ($r = 115.2$ mm, $l = 52$ mm) the peak voltage in the 50Ω load measures $V_{110}^{out}(\delta x) \approx 155$ mV/mm for a 1 nC bunch.

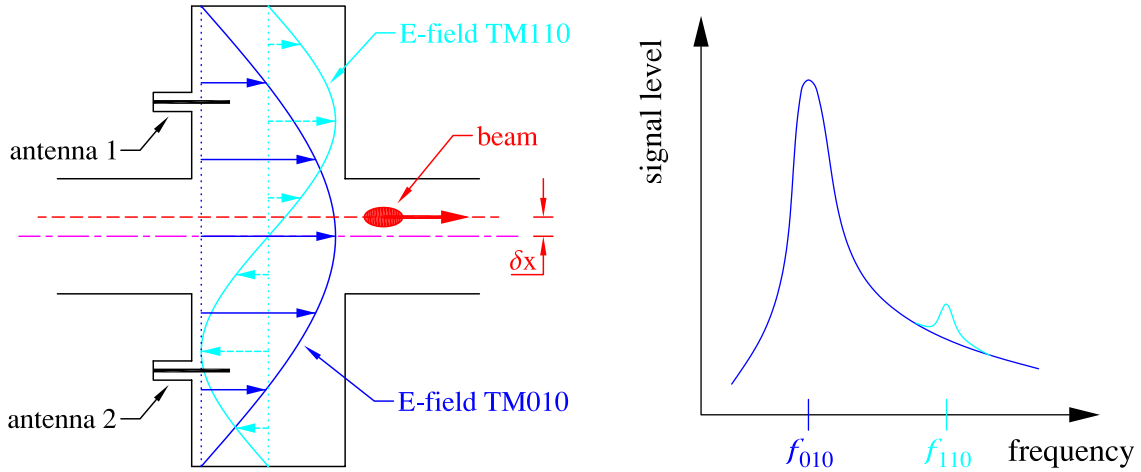


Figure 3: Excitation of the TM_{010} -mode (monopole) and the TM_{110} -mode (dipole)...
...and the corresponding signals in the frequency-domain.

Besides the TM_{110} -mode at 1.5167 GHz many other modes are excited, from which the TM_{010} monopole mode at 1.030 GHz dominates (see Figure 3). To suppress the unwanted signals, two pin-antennas for each plane are arranged symmetrically in the cavity monitor. Their signals are combined with a Δ/Σ -hybrid and further processed with a bandpass filter. With this techniques, followed by a *homodyne receiver* as read-out normalization electronics [3] a single bunch resolution of 20 μm could be verified at the TTF [4].

In order to resolve a single-bunch detection at the TTF with currently 1 μs bunch-to-bunch spacing, the quality factor of the cavity monitor had to be reduced to $Q_L \approx 1000$ by introduction of conductive wall losses (resonator material: stainless-steel). But this method is limited for the operation in the TESLA main linacs because of the high total heat load dissipated by all the 2×368 cavity monitors into the cryogenic system. Therefore high-Q copper-plated BPM resonators have to be used in TESLA, which then require some external damping – lowering the loaded Q – for a true single-bunch BPM detection. This can be realised by increasing the coupling of the 4 antennas, e.g. larger inductive loops instead of short capacitive pins.

An alternative concept tested in the TTF are the so-called *re-entrant* coaxial cavity monitors, where a broadband waveguide mode is used for to monitor the beam position:

3.1.2 Re-entrant Cavity BPM

A broadband re-entrant coaxial cavity BPM is proposed as alternative to the pillbox rf-cavity monitors in the TESLA main linacs (inside the cryomodules). It is also foreseen as high-resolution BPM detector for the fast luminosity feedback system. The re-entrant cavity consists out of the beam-pipe surrounded by another tube forming a piece of coaxial transmission-line (see Figure 4). At the upstream end this coaxial cylinder is excited by the EM-fields of the bunched beam passing through a concentric gap, at the downstream end it is shortened. Position sensitive signals are sensed with 4 symmetrical arranged feedthroughs at the upstream end of the coaxial structure.

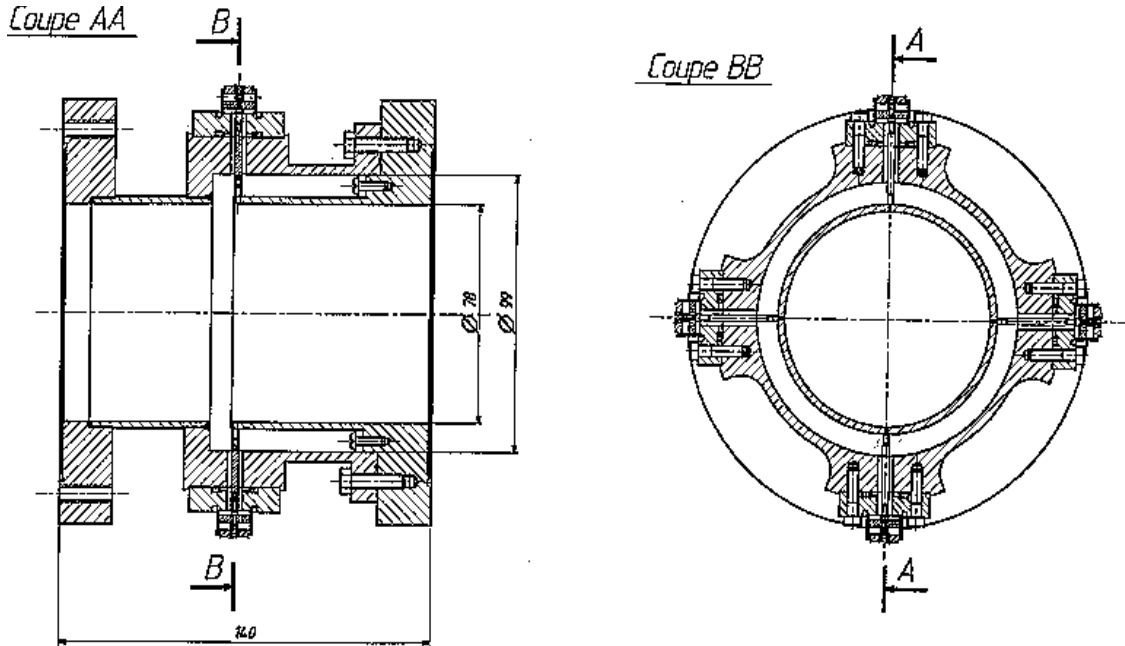


Figure 4: Re-entrant coaxial cavity monitor manufactured for the TTF

Instead of operating the re-entrant cavity at a narrow-band cavity dipole mode (which would be also possible), we monitor the evanescent fields of the beam excited fundamental TE_{11} waveguide dipole mode. The frequency of this mode is much lower (approximately the half) and it offers a

very large bandwidth (typically ≈ 100 MHz), thus gives high signal levels. Details on the theory of the re-entrant coaxial cavity are found in [5, 6, 7].

The actually used passband frequency and its bandwidth is defined by a bandpass filter (Bessel characteristic) in the pre-processing electronics. It is tuned to limit the time-domain response to 300 ns...10 μ s for the BPM's in the main linac cryo-modules, and down to 20 ns, required for the IR-BPM's. This is obtained without much degradation of the resolution in the presence of the very short bunches (1 ps) in TESLA. The filter bandwidth defines not only the measurement or integration time, but also the signal levels and therefore the signal-to-noise (S/N) ratio, i.e. the BPM-resolution. Further BPM development is under consideration to find the best compromise between space- and time resolution.

Other features of the broadband re-entrant cavity [6, 8] are:

- simple machineable mechanics.
- relative small dimensions.
- operation at cryogenic temperatures (2 K).
- moderate operation frequency w.r.t a narrow-band pillbox cavity.
- high resolution potential of the broadband waveguide mode (≈ 10 μ m in the TESLA main linacs).
- linearity errors < 1 % for the position measurement.
- low beam coupling impedance (low wake potentials) reduces the beam break-up forces in long bunch trains and minimizes the cryogenic heat-load due to resonances.

Five such BPM's are installed in the TTF [9]. The resolution is 10 μ m at 1 nC/bunch (calculated from the measured S/N-ratio) using bandpass filters with 8 MHz bandwidth. One BPM operates in the cryomodule of the capture cavity at 2 K.

Fabrication of the TTF re-entrant cavity Because of the axial symmetry a high precision is obtained by manufacturing the TTF re-entrant (Figure 4) cavity with a lathe. Small tolerances were applied on the radii, and the perpendicularity of the assembling surface. The concentricity actually measured on the cavities built for TTF was better than 20 μ m. The cavity was designed such, that it is simply to be demounted.

The commercial feedthroughs are UHV tight and applicable for 2 K cooling. They are well matched 50 Ω SMA types, showing a SWR below 1.02 at the operation frequency. The antenna tips are attached to the inner (beam-pipe) part of the coaxial cavity having a reliable electrical conduction. The cylindrical symmetry of the cavity and the outer positioning of the antenna facilitate cooling down to 2 K without stress.

Results on TTF and proposed parameters for the Tesla re-entrant BPM's In Table 3 the parameters of the re-entrant BPM's proposed for the TESLA main linac cryomodules and the fast feedback BPM detectors at the interaction point are given, and compared with results obtained at the TTF.

As the ratio *measurement range/single-bunch resolution* cannot exceed a value of a few 100, we have to accept a limited transverse measurement range for a 1 μ m single-bunch resolution for the fast feedback BPM's at the IR. In case of the main linac BPM's we reach the 5 μ m resolution by post-averaging the digitized BPM data within ≈ 10 μ s.

Experience and measurements at the re-entrant BPM located in the cryostat of the TTF capture cavity shows no problems at 2 K temperatures. When cooling down to 2 K, the cylindrical symmetry of the cavity was perfectly preserved. The resonance central frequency is shifted by a quantity much less than the bandwidth, so room temperature calibration remains valid.

	TTF BPM's (achieved)	main linac BPM's	IP BPM's
measurement mode	single-bunch	aver./single-bunch	single-bunch
# of BPM's	5	736	4
beam pipe diameter (mm)	78	78	48
length of the gap (mm)	8	8	5.5
active cavity length (mm)	50	50	40
total length incl. flanges (mm)	140	140	140
cavity outer diameter (mm)	200	200	180
operating frequency (MHz)	650	900	900
bessel filter bandwidth (MHz)	4 / 8	4	80
FWHM response time (ns)	260 / 130	260	13
measurement range (mm)	± 3	± 10	± 0.1
read-out electronics	superhet	AM/PM	superhet
integration time (ns)	400 / 200	10 000	20
resolution@3.2 nC/bunch (μm)	10	5	1

Table 3: Parameters of the re-entrant monitors testes in the TTF and proposed for TESLA

The read-out electronics for the TESLA re-entrant BPM's need to be simplified w.r.t. those tested on TTF in the following way (see section 4). For all re-entrant BPM systems a hybrid coupler with excellent isolation (> 50 dB over the whole bandwidth), located inside the tunnel as done at the TTF, could be necessary to reach the maximum resolution.

3.2 Stripline Monitors

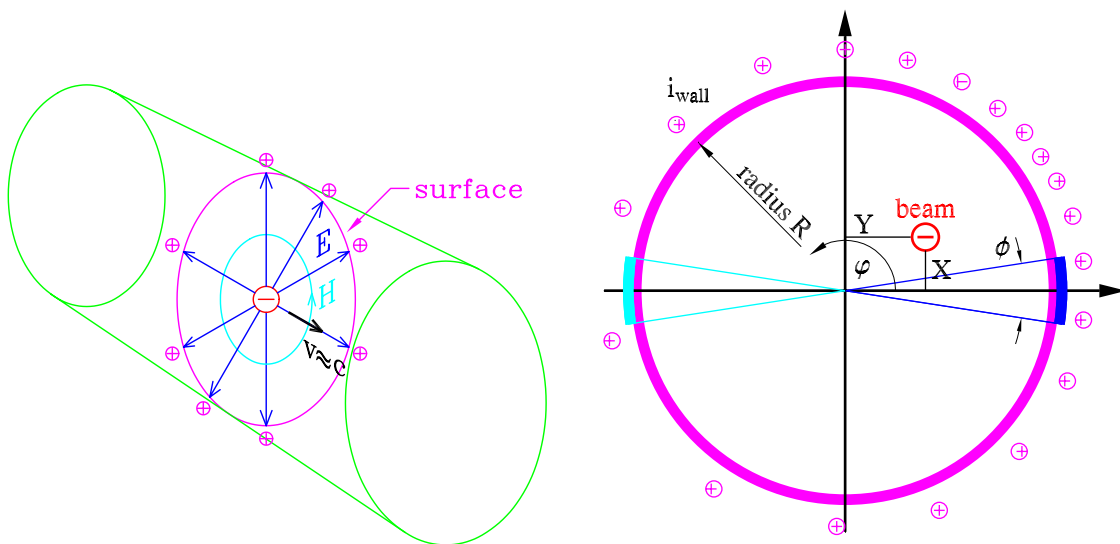


Figure 5: Image charges on the vacuum chamber...
...and wall current detection with two symmetrically arranged “ideal” electrodes.

Button as well as *stripline* electrodes are non-resonating, broadband pickup devices. The electromagnetic field of the beam is – in first order – not disturbed, therefore the *image charges* (or *wall currents*) on the unperturbed beam pipe can be analyzed to extract the pickup sensitivity. A part

ϕ of the wall currents

$$i_{\text{wall}}(\varphi) = -\frac{i_{\text{beam}}}{2\pi} \frac{1 - x^2 - y^2}{1 + x^2 + y^2 - 2x \cos \varphi - 2y \sin \varphi} \quad (6)$$

is sensed with two symmetrically arranged electrodes (see Figure 5). For normalized beam displacements ($x = X/R, y = Y/R$) this integrated wall currents on one electrode is given by (circular beam-pipe):

$$i_{\text{elec}} = -i_{\text{beam}} \frac{2}{\pi} f(x, y, \phi)$$

$$f(x, y, \phi) = \arctan \frac{[(1+x)^2 + y^2] \tan \phi / 4 - 2y}{1 - x^2 - y^2}$$

The normalized (beam intensity independent) position characteristic of two horizontal arranged electrodes can be expressed as ratio:

$$\frac{i_{\text{elec-right}}}{i_{\text{elec-left}}} = \frac{f(x, y, \phi)}{f(-x, y, \phi)} \quad (7)$$

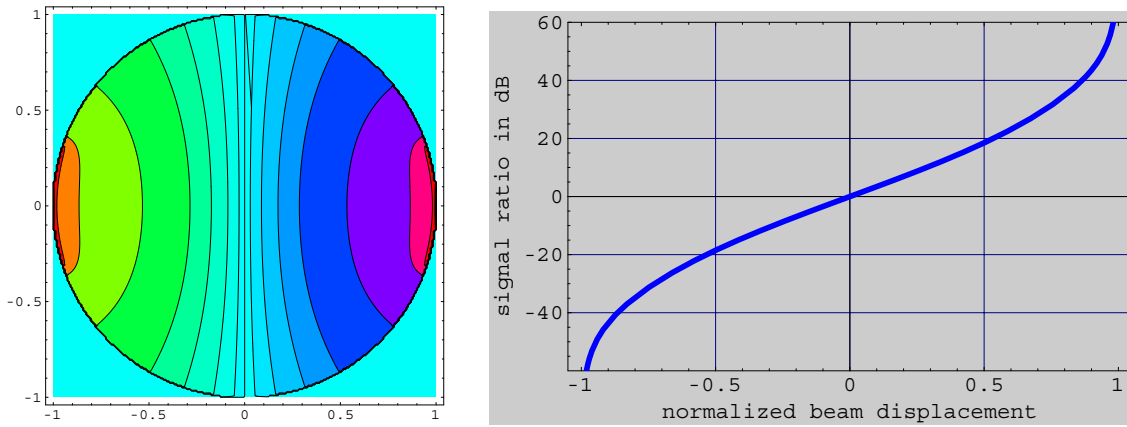


Figure 6: Position characteristics from the wall current model for a horizontal pickup ($\phi = 18^\circ$)

The contour plot $20 \log_{10} (i_{\text{elec-right}}/i_{\text{elec-left}})$ of eq.7 (Figure 6) shows lines of constant signal ratio: 0, ± 1 , ± 3 , ± 6 , ± 10 , ± 20 , ± 40 and ± 60 dB.

By moving only along the horizontal axis ($y=0$) one finds the normalized position characteristic (Fig. 6 right). Around the center of the beam pipe the position sensitivity is ≈ 20 dB/half aperture.

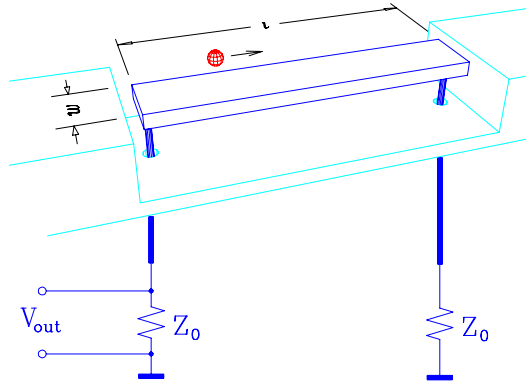


Figure 7: Stripline electrode.

Beside the beam position or displacement characteristic the *transfer characteristic* of a BPM pickup station is of major concern. The electrode of a stripline monitor consists out of a piece of *transmission-line* of length l which couples to the beam (width w) and is terminated at both ports in its characteristic impedance (see Figure 7).

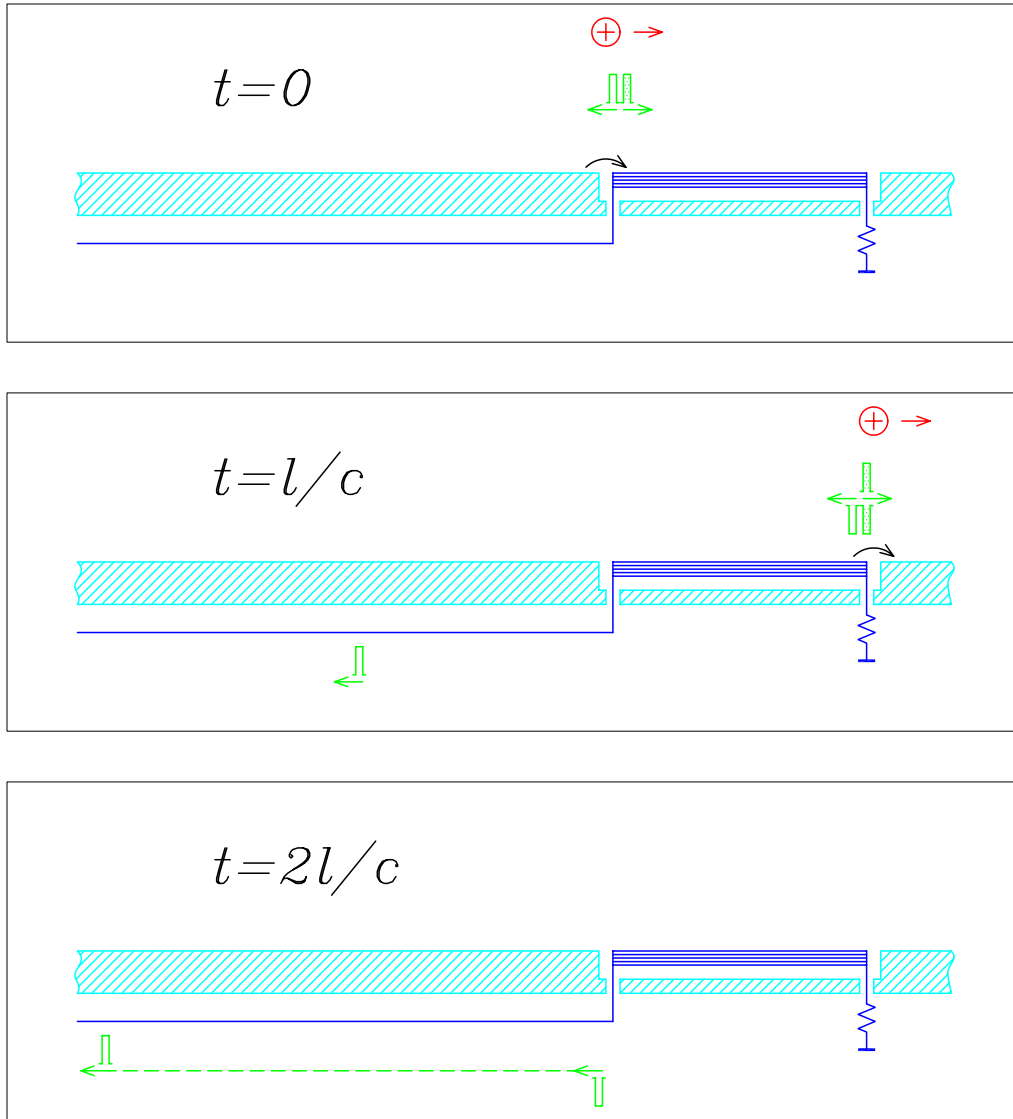


Figure 8: Operation principle of the stripline monitor.

A relativistic bunch charge ($v = c$), entering the upstream end of the stripline electrode (Figure 8, $t = 0$), generates a dirac impulse δ which splits in equal parts: one travelling via the output port along the attached cables, the other travelling synchronous with the charge along the stripline (hatched). As the charge arrives the downstream end of the electrode ($t = l/c$) it generates another dirac impulse with inverse polarity $-\delta$, which also splits: one part travels via the stripline electrode to the upstream port, the other compensates the just incoming dirac signal so there is no signal contribution at the downstream port! At the upstream port a dirac doubled pulse, spaced by $2l/c$ is generated, giving the time-domain *impulse response* of the stripline monitor:

$$h(t) = \frac{1}{2} \left[\delta(t) - \delta\left(t - \frac{2l}{c}\right) \right] \quad (8)$$

It is sensitive to the “directivity” of the beam. Eq.8 corresponds to a frequency domain *transfer function* of (see also Figure 9):

$$H(\omega) = j e^{-j\frac{\omega l}{c}} \sin\left(\frac{\omega l}{c}\right) \quad (9)$$

The maximas of the magnitude response are at the *center frequencies*: $f_c = (2n - 1)c/4l$

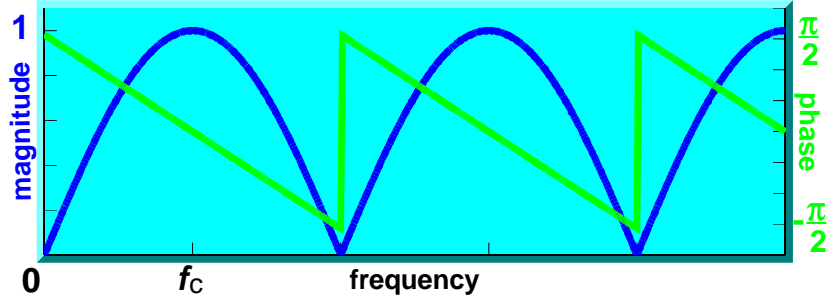


Figure 9: Frequency-domain transfer function of a stripline monitor.

Usually the stripline pickup operates at the first “lobe” (n=1). Its 3dB-bandwidth exceeds an octave: $f_{hi} = 3 f_{lo}$, $f_{lo} = f_c/2$.

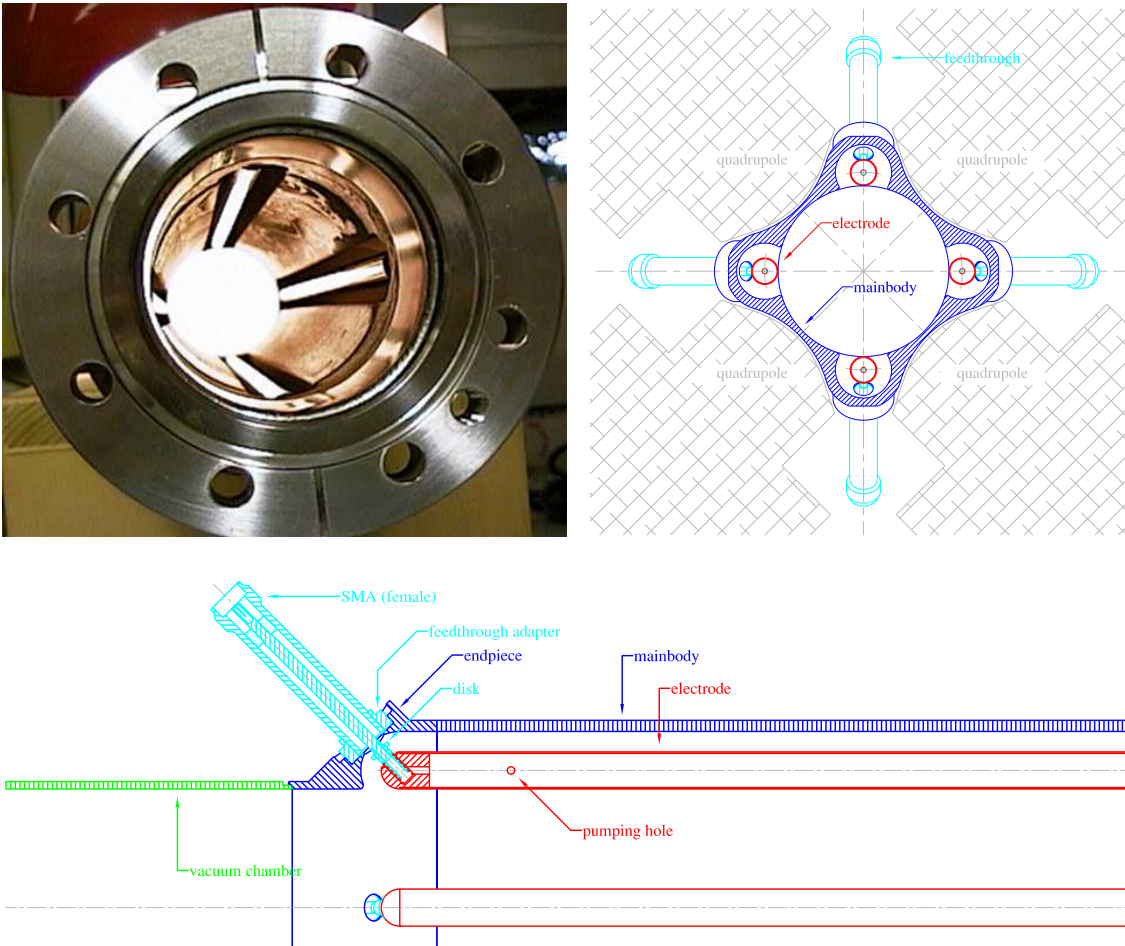


Figure 10: Stripline monitor with longitudinal slotted coaxial-lines.

Stripline monitors were successfully tested at the TTF [10, 11] and in many other accelerators on the DESY site [12]. In connection with AM/PM read-out electronics a single-bunch resolution of $20\ \mu\text{m}$ shows up in the 78 mm diameter beam-pipe of the TTF linac [13]. During the *Final Focus Test Beam* (FFTB) studies at SLAC a $1\ \mu\text{m}$ single-bunch resolution (!) [14] could be achieved with a dedicated stripline BPM system [15]. A similar BPM pickup [16] – original developed for DESY’s *S-Band Test Facility* (SBTF) – is equipped with four, well impedance-matched, 20 cm long stripline electrodes and fits inside the poles of a quadrupole magnet (Figure 10). Magnet and pickup were calibrated (aligned) with the same wire-measurement setup, which could specify the offset between quadrupole and pickup axes within an error margin of $20\ \mu\text{m}$ [17]. The stripline electrodes itself are realized as longitudinal slotted coaxial-lines, which minimizes the reflexions at the transitions of the ports (feedthroughs).

Although the stripline monitor is of more complicated mechanics w.r.t. a button monitor, it has several advantages for precision beam position monitoring:

- High output levels in the medium RF range (250...500 MHz) simplifies read-out electronics and minimizes the S/N-ratio: enhanced position resolution.
- $50\ \Omega$ source impedance simplifies input filters and reduces reflexions in the BPM system.
- Downstream ports can be used to supply interleaved calibration signals.

The stripline monitors proposed for the BDS and the FEL-undulators of TESLA will be basically of similar shape and characteristics to that in Figure 10. Because of the small beam-pipe aperture in the FEL-undulators some modifications (re-development) have to be applied. Two more stripline monitors are required as BPM detector for the fast luminosity feedback system. Their location is $\approx 3\ \text{m}$ on each side of the IR, before the beam separation. Here we profit from the directivity of the stripline monitor, so a 10 ns measurement time is *not required* for the independent single-bunch BPM detection of both beams.

At locations where maximum position resolution is of less interest (e.g. injector complex, transport lines, etc.) the more cost effective button monitors are preferred. Because of the averaging possibilities this pickup type can also be used in the damping rings as high resolution BPM.

4 Read-out Electronics

For maintenance and manpower reasons the number of different electronics installations, which has to read-out the BPM’s of the TESLA accelerator complex, has to be limited. Therefore we split the *BPM signal processing* in a pickup type specific *pre-processor*, followed by the actual normalizing read-out electronics. (Figure 11).

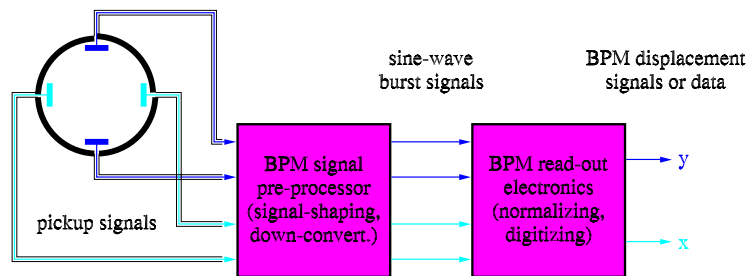


Figure 11: Splitted BPM signal processing: pre-processor and normalizer

The pre-processor modifies/shapes the pickup electrode signals such that the normalizing read-out electronics can handle them. In case of button or stripline BPM’s it consists simply out of two pairs of matched passive low-pass or band-pass filter networks. For a cavity BPM a more complex downconverter circuit (band-pass filter, variable gain amplifier, mixer, LO, etc.) has to

be implemented. In both cases the 4 output signals of the pre-processor are still beam-intensity and beam-position dependent. For a single bunch passage it outputs sine-wave burst signals of 10...40 oscillations in the 100...400 MHz frequency range, which are simple to be processed by the normalizing electronics.

From the different BPM signal processing principles [18, 19] available, the following two read-out systems will cover nearly all BPM requirements at TESLA:

4.1 AM/PM BPM Signal Processing

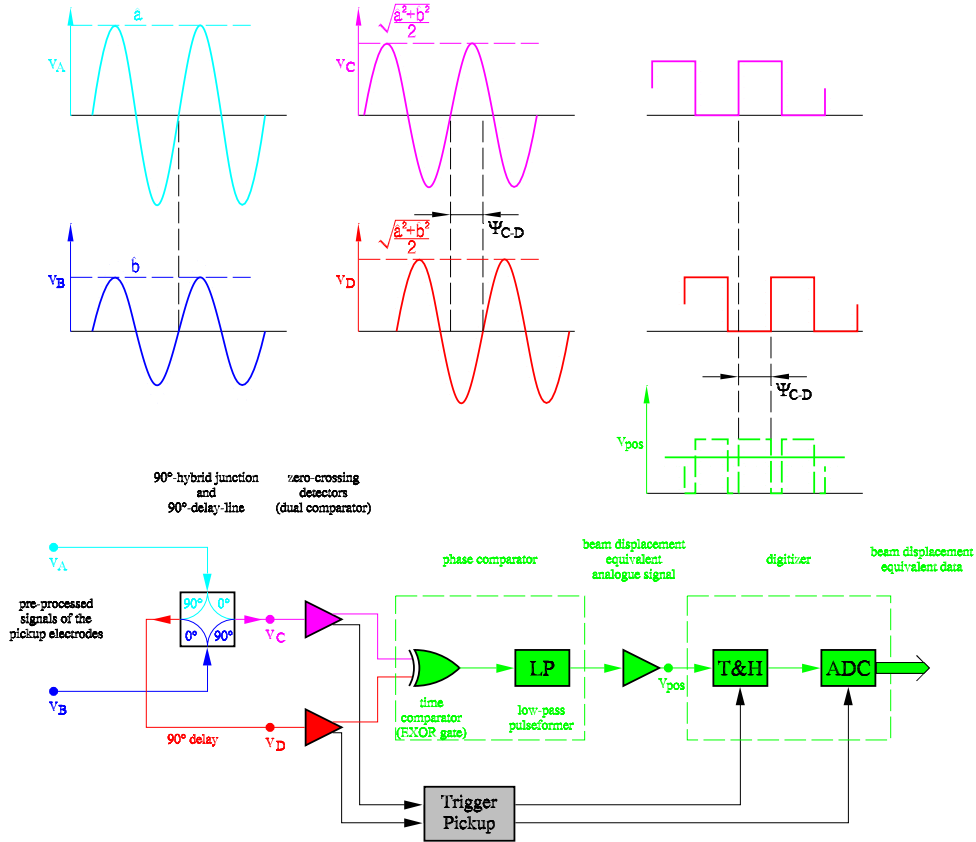


Figure 12: AM/PM signal processing.

For each plane (horizontal or vertical) the corresponding BPM pickup electrodes supplies two signals (A and B). Their *amplitude-ratio* \hat{a}/\hat{b} is a beam-intensity independent function of the beam displacement:

$$\text{beam-position} = f\left(\frac{\hat{a}}{\hat{b}}\right) \quad (10)$$

The amplitude-ratio, and such the beam-position, is measured with the *AM/PM signal processor* by converting the ratio into a phase-difference – the *amplitude modulation* (AM) converts into a *phase modulation* (PM). The conversion is realized by a 90° hybrid junction, which is extended at one output port with a 90° delay-line (see Figure 12).

It is sufficient to analyse the sine-wave burst signals of the pre-processor as stationary sine-wave voltage functions v_A and v_B :

$$v_A(t) = \hat{a}e^{j\omega t} \quad (11)$$

$$v_B(t) = \hat{b}e^{j\omega t} \quad (12)$$

They have same the frequency and are in phase, but the amplitudes \hat{a} and \hat{b} differ due to the beam displacement and are bunch charge dependent. At the outputs C and D of the hybrid/delay circuit the signals:

$$v_C(t) = \sqrt{\frac{\hat{a}^2 + \hat{b}^2}{2}} \arctan \left[\frac{\hat{a} \sin(\omega t) + \hat{b} \cos(\omega t)}{\hat{a} \cos(\omega t) - \hat{b} \sin(\omega t)} \right] \quad (13)$$

$$v_D(t) = \sqrt{\frac{\hat{a}^2 + \hat{b}^2}{2}} \arctan \left[\frac{\hat{a} \sin(\omega t) - \hat{b} \cos(\omega t)}{\hat{a} \cos(\omega t) + \hat{b} \sin(\omega t)} \right] \quad (14)$$

have the same amplitude, but as Figure 12 illustrates, the amplitude-ratio of A and B is converted into a phase-difference (see also Figure 13):

$$\Psi_{C-D} = 2 \operatorname{arccot} \left(\frac{\hat{a}}{\hat{b}} \right) \quad (15)$$

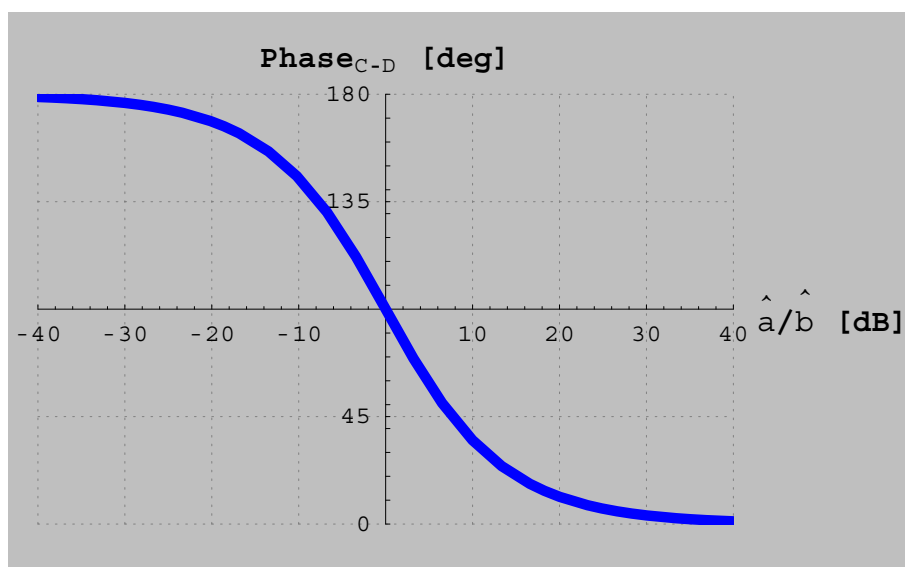


Figure 13: Amplitude-ratio to phase-difference conversion of the hybrid/delay circuit.

Following the schematics in Figure 12, both sine-wave burst signals v_C and v_D are “digitized” with a dual analogue comparator (1-bit):

This comparator acts as zero-crossing detector, it’s digital output returns a logic-high for positive input voltages and a logic-low for negative ones (see also the diagrams in Figure 12). At this point the two digital signals are independent of the bunch charge.

The actual beam displacement is deduced with the following digital phase comparator circuit. It consists out of an EXOR gate which delivers a pulse width “modulated” signal, containing the beam position information. A lowpass filter network averages for an analogue pulse signal, which now remains as pure beam position dependent signal v_{pos} .

After some amplification, the time- and amplitude-quantization (digitizing) take place with the usual track&hold amplifier (T&H) and analogue-to-digital converter (ADC) combination. Clock/trigger signals for these circuits may be supplied internally from the analogue comparator, or from an external timing system.

The AM/PM BPM signal processing was introduced first in the *Tevatron* (FNAL) as narrow bandwidth system [20]. The single bunch capability was added in the installations at *LEP* (CERN) [21] and *HERA-p* (DESY) [22]. The successful operation in those large scale, high energy particle accelerators are due to some major advantages of the AM/PM BPM read-out method:

- The full beam displacement range is covered, including a large dynamic range (> 40 dB) of beam/bunch intensities, without attenuator/amplifier switching.
- The AM/PM method offers a reliable beam position measurement also at small beam displacements, when subtraction methods (e.g. Δ/Σ signal processing) may fail.
- The AM/PM BPM electronics can be divided into a few simple basic subcircuits: passive networks, linear amplifiers, digital gate functions and analogue comparators. There is no manufactur dependence for high integrated, specialized semiconductor circuits.
- All the needed semiconductors and parts are available in radiation resistant(!) bipolar process technology. The electronics can be installed in the accelerator tunnel!

At the TTF linac stripline BPM signals were successfully processed with AM/PM read-out electronics [13, 24]. With the latest high-speed (> 3 GHz bandwidth) logic gate families (*ON semiconductor* ECLinPS Plus) a monopulse (single oscillation) AM/PM signal processor was developed for button electrode pickups, serving the FEL-undulator BPM's at TTF (DESY). This improved AM/PM technique will also be used for the BPM system of the LHC (CERN) [23].

4.2 Digital BPM Signal Processing

The AM/PM method, as well as most of the other BPM read-out principles, uses analogue signal processing schemas to extract a normalized displacement signal from the original electrode signals of the pickup. This pure beam position dependent, single-bunch signal is well amplified and “stretched” in time to be simply digitized with a single clock impulse at the ADC.

In case of the *digital* BPM read-out system the electrode signals are digitized individually. 4 digital receiver channels, each including an ADC, are used to acquire the signals of a BPM pickup with two horizontal and two vertical arranged electrodes. Each channel measures the signal level of “his” electrode using digital data acquisition techniques, then the horizontal and vertical beam positions are calculated in real-time with the attached *digital signal processor* (DSP). A sine-wave burst pre-processing of the electrode signals (see at the beginning of section 4) has to be realized before the digitizing takes place. In order to meet the TESLA resolution requirements in space and time(!), each receiver channel has to offer:

- A sufficient dynamic range for beam intensity/displacement variations of the pre-processed output signals of the pickup electrodes, eq.(1).
- Sufficient sampling speed, operation throughput and analogue bandwidth to guarantee a single-bunch processing

The sine-wave amplitudes are measured (demodulated) by applying *orthogonal* sampling. This principle is based on the fact that the amplitude A of two orthogonal sine-wave functions

$$I = A \cos(\omega t + \varphi) \quad (16)$$

$$Q = A \sin(\omega t + \varphi) \quad (17)$$

is given by the squareroot of the sum of the squares of inphase I and quadruphase Q components:

$$A = \sqrt{I^2 + Q^2} \quad (18)$$

Therefore the sampling rate of the ADC of the digital BPM receiver is adapted to the frequency of the sine-wave burst signals applied at the input (see Figure 14). Equidistant samples are taken with 90° phase-advance, but sampling may be completely asynchronous to the signal phase φ . The following signal processing steps are implemented purely digital:

The digitized signal-data is ordered into inphase I and quadruphase Q components, which are demodulated separately using a *numerically controlled oscillator* (NCO). The NCO frequency is set to that of the sine-wave burst, feeding this reference frequency into the I and Q synchron

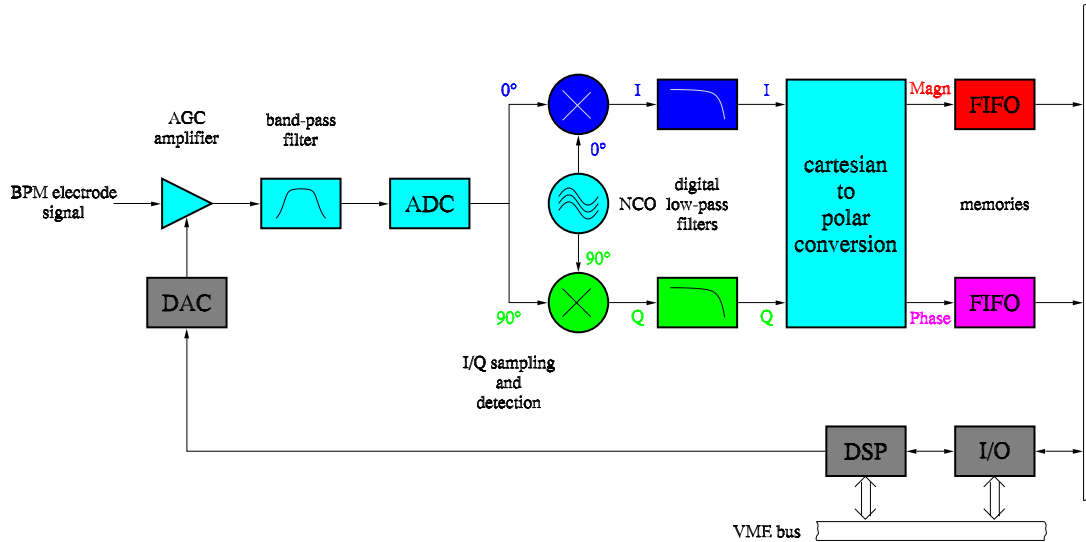


Figure 14: One channel – out of four – of a digital BPM receiver (principle schematics without clock and timing details).

detectors. Not only the amplitude *Magn* of the input signal is derived in the following coordinate conversion section, but also its *Phase*. The data of all four digital BPM receiver channels is sent to the attached DSP to be analyzed for the horizontal and vertical beam displacement.

The digital BPM receiver was introduced first time at the *Swiss Light Source* (PSI) [25]. The technology is now available from industry in a VME environment [26]. Basis of the digital BPM receiver is the digital IF technology applied in commercial communication systems, such as cellular phones, GPS receivers, etc. A pipelined ADC with a resolution of 12-bit or more is a central part in these systems. With the latest ADC developments – offering > 70 dB S/N ratio, > 100 MS/s sampling rate, > 250 MHz analogue bandwidth, etc. – a digital BPM read-out system seems to be feasible for TESLA. *Automatic gain controlled* (AGC) amplifiers (controlled by the DSP) in front of the ADC and in the pre-processing electronics, further extend the dynamic range of each receiver channel. In the TESLA BPM pre-processing electronics a broadband Bessel or Gauß band-pass filter with a center frequency of ≈ 50 MHz would define a sine-wave burst signal of 10...15 oscillations for a single bunch passage. This would give > 10 useable data samples for each plane (*I* and *Q*) per bunch and channel, which is sufficient for a single-bunch BPM I/Q detection.

Main advantages of the digital BPM read-out electronics are:

- No switched elements in the rf-path.
- The I/Q detection offers amplitude and phase information (redundance) of the measured signals.
- Sophisticated real-time algorithms (calibration, statistics, FFT, wavelets, etc.) can be applied by re-programming of the DSP to improve BPM resolution and accuracy.
- Continuous-wave (CW) calibration signals can be superimposed to the BPM electrode signals. The low-level CW calibration harmonic is simply to distinguish from the broadband BPM signals with a FFT-algorithm.
- Most modifications (re-calibration, averaging, etc.) are software-based and simple to arrange, no tunnel access required!

Beside all these positive aspects, the hardware of the digital BPM electronics is based on CMOS technology, which is **not** radiation tolerant! This shielding problem, as well as many other questions are currently studied at the TESLA Test Facility linac

References

- [1] R. Brinkmann, “The TESLA Linear Collider”, Linear Collider Workshop LCWS 99, Sidges, Spain ; April 1999.
- [2] R. Lorenz, Dissertation, TU Berlin, 1996, unpublished (in german).
- [3] R. Lorenz, “Cavity-Monitors at the TESLA Test Facility Linac”, DESY, December 30, 1999, unpublished.
- [4] H. Weise, DESY dept. MIN, private communications.
- [5] R. Bossart , “Beam Position Monitor Using a Reentrant Coaxial Cavity”, PS/LP Note 91-19, CERN, Geneva, Switzerland; June, 1991.
- [6] R. Bossart , “Microwave Beam Position Monitor Using a Re-entrant Coaxial Cavity”, CERN PS 91-59 (LP) CLIC Note 174, CERN, Geneva, Switzerland; August, 1992.
- [7] R. Bossart , “High Precision Beam Position Monitor Using a Re-entrant Coaxial Cavity”, Proc. of the 17th International Linac Conference LINAC 94 , Tsukuba, Japan; August 21 - 26, 1994.
- [8] C. Magne, et al., “High Resolution BPM for Future Linear Colliders”, Proc. of the 19th International Linac Conference LINAC 98, Chicago, IL, USA; 1998.
- [9] M. Juillard, C. Magne, A. Mosnier, B. Phung, “High Resolution BPM For The Next Linear Colliders”, 9th Beam Instrumentation Workshop BIW '00, MIT Bates, Cambridge, MA, USA; May 8 - 11, 2000.
- [10] R. Lorenz, et al., “Measurement of the Beam Position in the TESLA Test Facility Linac”, Proc. of the 18th International Linac Conference LINAC 96, Geneva, Switzerland; August 26 - 30, 1996.
- [11] P. Castro, P. Patteri, F. Tazzioli, “Experience with Stripline Beam Position Monitors on the TESLA Test Facility Linac”, Proceedings of the 4th European Workshop on Diagnostics and Instrumentation for Particle Accelerators DIPAC 99, Chester, UK ; May 16 - 18, 1999.
- [12] W. Schütte, M. Wendt and K. H. Meß, “The New Directional-Coupler Pick-Up for the HERA Proton Beam Position Monitoring System”, Proc. of the 12th IEEE Particle Accelerator Conference PAC 87, Washington D.C., USA; March 16 - 19, 1987.
- [13] L. Cacciotti, P. Patteri, F. Tazzioli, “The New Front End Module of the TTF Stripline BPM Detector with Single Bunch Response”, TESA 98-18; DESY, Hamburg, Germany; July 1998.
- [14] M. Ross, “Frontiers of Accelerator Instrumentation”, Proc. of the Advanced Accelerator Concepts Workshop, Port Jefferson, Long Island, NY, USA; June 14 - 20, 1992.
- [15] J.-C. Denard, et. al., “Monitoring the Beam Position in the SLC Interaction Region”, Proc. of the 12th IEEE Particle Accelerator Conference PAC 87, Washington D.C., USA; March 16 - 19, 1987.
- [16] W. Radloff and M. Wendt, “Beam Monitors for the S-Band Test Facility”, Proc. of the 16th IEEE Particle Accelerator Conference PAC 95, Dallas, TX, USA; May 1 - 5, 1995.
- [17] F. Brinker, A. Hagestedt, M. Wendt, “Precision Alignment of BPM's with Quadrupole Magnets”, Proc. of the 18th International Linac Conference LINAC 96, Geneva, Switzerland; August 26 - 30, 1996.
- [18] G. Vismara, “The Comparision of Signal Processing Systems for Beam Position Monitors”, Proceedings of the 4th European Workshop on Diagnostics and Instrumentation for Particle Accelerators DIPAC 99, Chester, UK ; May 16 - 18, 1999.

- [19] G. Vismara, “Signal Processing for Beam Position Monitors”, 9th Beam Instrumentation Workshop BIW '00, MIT Bates, Cambridge, MA, USA ; May 8 - 11, 2000.
- [20] R. E. Shafer, et. al., “The Tevatron Beam Position and Beam Loss Monitoring System”, Proc. of the International Conference of High Energy Accelerators HEACC 88, FNAL Batavia, IL, USA; 1988.
- [21] J. Bosser, L. Burnod, G. Feroili, “Beam Position Measurements by Use of 90⁰ Hybrids (Proposal for LEP)”, CERN SPS/ABM/83-01/00586, January 1983.
- [22] A. Jacob, et. al., “The HERA-p BPM Readout System”, Proc. of the 2th European Particle Accelerator Conference EPAC 90, Nice, France; August 16 - 18, 1990.
- [23] D. Cocq, “The wide band normalizer – a new circuit to measure transverse bunch position in accelerators and colliders”, Nuclear Instruments & Methods in Physics Research A 416 (1998) 1 - 8.
- [24] M. Castellano, et. al., “TESLA Test Facility Stripline Readout System”, Proc. of the 5th European Particle Accelerator Conference EPAC 96, Sidges, Spain; June 10 - 14, 1996.
- [25] M. Dehler, et. al., “New Digital BPM Systems for the Swiss Light Source”, Proceedings of the 4th European Workshop on Diagnostics and Instrumentation for Particle Accelerators DIPAC 99, Chester, UK ; May 16 - 18, 1999.
- [26] Instrumentation Technologies, “Quad Digital Receiver QDR”, brochure of the company.